Geoderma 429 (2023) 116227

Contents lists available at ScienceDirect

Geoderma

journal homepage: www.elsevier.com/locate/geoderma

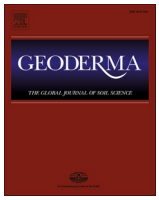

Phosphorus species in sequentially extracted soil organic matter fractions

Jolanda E. Reusser [a,b,*], Alessandro Piccolo [c], Giovanni Vinci [c], Claudia Savarese [c], Silvana Cangemi [c], Vincenza Cozzolino [c], René Verel [d], Emmanuel Frossard [a], Timothy I. McLaren [e]

[a] Department of Environmental Systems Science, ETH Zurich, 8315 Lindau, Switzerland
[b] Swiss Soil Monitoring Network NABO, Agroscope, 8046 Zurich, Switzerland
[c] Interdepartmental Research Center on Nuclear Magnetic Resonance for the Environment, Agro-Food and New Materials (CERMANU), University of Napoli Federico II, 80055 Portici, Italy
[d] Department of Chemistry and Applied Biosciences, ETH Zurich, 8093 Zurich, Switzerland
[e] School of Agriculture and Food Sciences, University of Queensland, 4072 St Lucia, Australia

ARTICLE INFO

Handling Editor: Andrew Margenot

Keywords:
Soil organic matter
Solution ^{31}P NMR spectroscopy
Sequential chemical fractionation
Phosphomonoester
Inositol phosphate
Organic phosphorus

ABSTRACT

The majority of organic P (P_{org}) in soil is considered to be part of soil organic matter (SOM) associations, but its chemical nature is largely 'unresolved'. In this study, we investigated the P_{org} composition in different SOM fractions of a Gleysol soil using the Humeomics sequential chemical fractionation (SCF) procedure combined with nuclear magnetic resonance (NMR) spectroscopy.

In summary, SCF procedure with subsequent NaOH-EDTA extraction of the soil residue extracted a total of 1769 mg P/kg$_{soil}$ compared to 1682 mg P/kg$_{soil}$ of a single-step NaOH-EDTA extraction. Approximately 38 % of the extracted P_{org} was present in the form of the unresolved P_{org} pool, which was represented by one or two underlying broad signals in the phosphomonoester region of solution ^{31}P NMR spectra. The SCF revealed that phosphomonoesters were recovered in each fraction: 47 % of the unresolved phosphomonoesters were associated with the SOM fraction released by breaking ester bonds (40 %) and ether bonds (7 %), whereas about 30 % of this unresolved P_{org} pool appeared in the SOM fraction closely associated with the soil mineral phase. Furthermore, the extractability of inositol phosphates (IP) was increased from 312 mg P/kg$_{soil}$ to 534 mg P/kg$_{soil}$ (factor 1.7) using the SCF procedure compared to a single-step NaOH-EDTA extraction. Previous studies have reported the presence of IP in molecular size fractions greater than 10 kDa. Our findings on the removal of IP with the fractionation of the SOM could explain the presence of IP in these large associations.

We demonstrate that major pools of P_{org} are closely associated with SOM structures, comprising a diverse array of chemical species and bonding types. These results forward our understanding of P_{org} stabilisation, P transformation, and P cycling in terrestrial ecosystems towards an association point of view.

1. Introduction

Phosphorus (P) is an essential component of the energy storing compounds, genome of living organisms, biological membranes, etc. Organic molecules containing P in soil, i.e. soil organic P (P_{org}), generally comprise between 20 % and 80 % of the total P in soil (Anderson, 1980). Soil P_{org} exists as P covalently bound to an organic moiety R (R–PO_3, phosphonates), via an ester linkage (R–O–PO_3, phosphomonoester), or via two ester linkages (R^1–O–PO_2–O–R^2, phosphodiesters) (Condron et al., 2005). In addition, soil P_{org} can include phosphate bound to soil organic matter (SOM) compounds through metal-bridges, or condensed forms of P (e.g. polyphosphates) present within microorganisms (George et al., 2018; McLaren et al., 2020).

The chemical nature of the majority of P_{org} in soil remains unresolved (McLaren et al., 2020). This 'unresolved' pool of P_{org} can be accounted for as an underlying broad signal in the phosphomonoester region of ^{31}P NMR spectra on soil extracts (McLaren et al., 2015; Reusser et al., 2020a). The molecules comprising the unresolved phosphomonoesters are of apparent large molecular weight, presumably complex in structure, and resistant to enzymatic hydrolysis (He et al., 2006; Jarosch et al., 2015; McLaren et al., 2020; McLaren et al., 2015). Furthermore, there is increasing evidence this pool contains several components of

* Corresponding author at: Department of Environmental Systems Science, ETH Zurich, 8315 Lindau, Switzerland.
E-mail address: jolanda.reusser@usys.ethz.ch (J.E. Reusser).

https://doi.org/10.1016/j.geoderma.2022.116227
Received 18 June 2022; Received in revised form 9 September 2022; Accepted 12 October 2022
Available online 27 October 2022

varying molecular weights rather than a single, large and polymeric macromolecule (McLaren et al., 2019).

The occurrence of unresolved phosphomonoesters in large molecular weight factions of alkaline (NaOH) soil extracts suggests a close association with apparently large SOM structures, because by definition, humic and fulvic acids are extracted with alkali from soil (Stevenson, 1994). For example, Ogner (1983) extracted humic acids from four Norwegian raw humus types using 0.5 M NaOH. The subsequent solution ^{31}P NMR spectroscopic analyses revealed a great diversity and abundance of phosphomonoesters in large molecular weight material of these humic acids. The close association of the unresolved phosphomonoesters with large structures of the organic matter was also hypothesised by Dougherty et al. (2007) and McLaren et al. (2015). Dougherty et al. (2007) reported that an underlying broad signal in the phosphomonoester region of ^{31}P NMR spectra on soil extracts partially resisted an HF treatment whereas phytate was completely removed. McLaren et al. (2015) attributed the presence of an underlying broad signal in the phosphomonoester region of ^{31}P NMR soil spectra in large molecular size material > 10 kDa to the unresolved P_{org} pool associated with large SOM structures. However, knowledge on the associations and bonding types of the unresolved phosphomonoesters with the SOM structures and mineral phase is very limited.

Inositol phosphates (IP) are another major pool of P_{org} in soils. They are the predominant pool of P in seeds, and can accumulate in soil due to their high sorption affinity to soil constituents (Celi and Barberis, 2007). Concentrations of IP vary widely in soil ranging from less than 1 % up to more than 80 % of the total pool of P_{org} in soil (Cosgrove and Irving, 1980; Harrison, 1987; McDowell and Stewart, 2006; Smernik and Dougherty, 2007). The most abundant IP form in soil is *myo*-IP_6, commonly known as phytate, followed by the *scyllo* isomer of IP_6 (Cosgrove and Irving, 1980; Turner et al., 2002). The other two isomers of IP (*neo*- and *chiro*) are less abundant in soil. Recently, Reusser et al. (2020b) reported that the diversity of IPs in soils is much higher than previously thought, based on solution ^{31}P NMR spectra of hypobromite oxidised soil extracts. Furthermore, the authors provided direct spectroscopic evidence for the existence of several lower-order IP species in soil extracts.

Pools of IP are largely considered to be associated with the mineral phase of soils, e.g. amorphous aluminium (Al) and iron (Fe) minerals, clay minerals, or calcite (Celi and Barberis, 2007; Celi et al., 1999; Turner et al., 2002). However, there is supporting evidence that IP can be associated with the organic phase of soils (Borie et al., 1989; Hong and Yamane, 1980; Moyer and Thomas, 1970). Furthermore, Jørgensen et al. (2015) indicated that the association of IP_6 with other SOM compounds can be important even in soils with high concentrations of amorphous Al and Fe minerals. The authors reported that more than half of IP_6 was associated with other SOM structures in strongly weathered Oxisols and one fourth in SOM rich grassland soils. Indeed, despite the apparent high abundance of these IP-SOM associations and the possible role of IP in the stabilisation of SOM due to its high sorption affinity to soil components (Celi and Barberis, 2007; Tipping et al., 2016), the types of these associations and the formation mechanisms are largely unknown.

Piccolo (2001) described SOM as an association of small molecules forming suprastructures of apparent large molecular size. These small molecules (not more than 400–1000 Da) are stabilised within the SOM suprastructure by various bonding types, including van der Waals and hydrogen bonds (Piccolo, 2001; Piccolo et al., 2019). Nebbioso and Piccolo (2011) developed the 'Humeomics' sequential chemical fractionation (SCF) procedure to fractionate the SOM using different extractants. These extractants are of increasing cleaving strength (decreasing base resp. acid dissociation constants), hence progressively breaking inter- and intramolecular bonds (e.g. C—O bonds) without breaking any C—C bonds (Nebbioso and Piccolo, 2011). In the Humeomics SCF procedure, extraction with a dichloromethane/methanol (DCM/MeOH) solution yields the 'unbound' SOM fraction, extraction with a 12 % (1.9 M) BF_3 in MeOH solution the 'weakly ester-bound', extraction with a 0.5 M KOH in MeOH solution the 'strongly ester-bound', and extraction with 47 % (11 M) HI the 'ether-bound' fraction according to the cleaving strength of the applied extractants (Nebbioso and Piccolo, 2011). The residual fraction is assumed to be closely associated with the mineral phase. In summary, the unbound fraction consists of free molecules and molecules liberated from associations held together by weak dispersive forces (Piccolo et al., 2019). Subsequently, readily accessible ester linkages are transesterified, giving rise to the operationally defined 'weakly' ester-bound fraction. In a next step, ester linkages are cleaved which were not physically accessible during the first transesterification process, resulting in the 'strongly' ester-bound fraction. In the last step, ether linkages are cleaved, resulting in the ether-bound and residual fractions. Drosos et al. (2017) applied the SCF procedure to an agricultural sandy loam soil and reported the extraction of 235 % more soil organic C compared to a single-step alkaline (0.5 M NaOH + 0.1 M $Na_4P_2O_7$) extraction. The authors found that most C was extracted from the SOM suprastructure by breaking the weak (32 %) and strong (16 %) ester linkages. The ether-bound fraction was minor, comprising 5 % of total C. The residue after the Humeomics SCF contained 39 % of total C. This final residue is assumed to consist mostly of SOM bound to the soil mineral matrix via two processes (Drosos et al., 2017): 1) adsorption of hydrophobic components on aluminosilicate surfaces and 2) complex formation between iron and oxygen containing hydrophilic groups.

In this study, we combine the SOM sequential fractionation method of Humeomics (Nebbioso and Piccolo, 2011) with solution ^{31}P NMR spectroscopy for P_{org} speciation (Cade-Menun, 2005; McLaren et al., 2020), in order to provide new insight on the chemical nature and associations of soil P_{org} with other SOM structures. The aim of this study was to fractionate the SOM suprastructures into smaller components with subsequent speciation of P_{org} compounds within the different fractions and the residues.

We hypothesise that: 1) the Humeomics SCF procedure will extract more soil P compared to a single-step NaOH-EDTA extraction due to enhanced accessibility of the compounds by the extractants caused by stepwise 'decoating' of the SOM structures; 2) subsequent fractionation of the SOM suprastructure causes a decrease in the pool of unresolved phosphomonoesters; and 3) the predominant bonding type for unresolved pools of P_{org} associated with large structures (suprastructures) of SOM is via ester linkages.

2. Materials and methods

2.1. Soil collection and preparation

A sample from a Gleysol (WRB, 2014) under pasture was collected in 2017 from the 0–10 cm layer in Switzerland. Detailed information on the location and soil properties can be found in Reusser et al. (2020a). The soil sample was sieved (<5 mm), dried for 5 days at 60 °C, and then ground to powder using a mortar and pestle to pass through a 0.5 mm sieve.

2.2. Humeomics sequential chemical fractionation

The Humeomics SCF procedure was carried out on three replicates of the Gleysol at the Institute of Agricultural Chemistry, University of Naples Federico II in Naples. One horizon of one soil (with three replicates) was chosen due to the time-consuming and expensive nature of the Humeomics SCF and NMR analyses. The SCF procedure is based on a slightly modified version of the method of Nebbioso and Piccolo (2011), which is summarised in Fig. 1. If not otherwise stated, extraction of soils occurred at room temperature (21 °C), centrifugation of extracts was carried out at 7500 rpm (8678 *g*) at 10 °C and the supernatant passed through a Whatman® no. 41 filter paper.

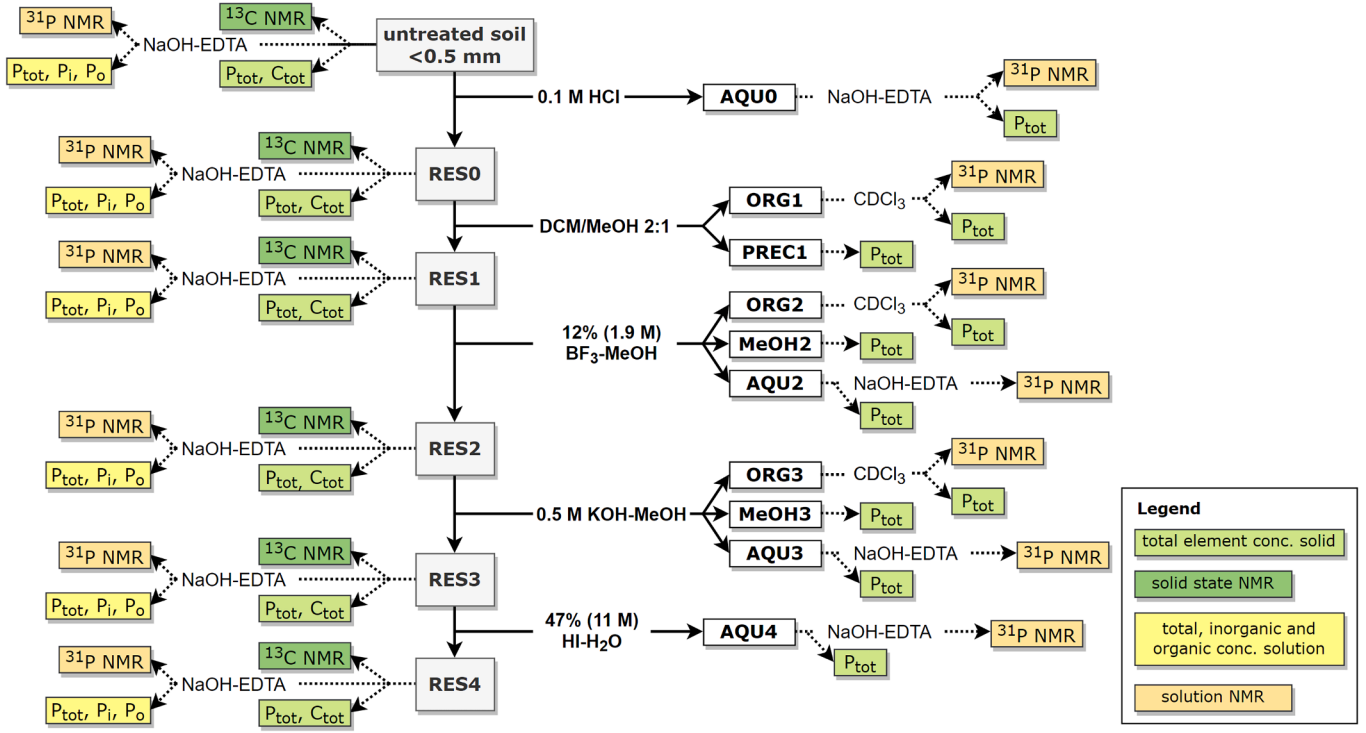

Fig. 1. A summary of the Humeomics sequential chemical fractionation procedure, as modified from Nebbioso and Piccolo (2011), and the different measurements taken on all samples. The term 'RES' refers to the dried soil residue after the respective extraction step, 'AQU' to the aqueous phase, 'ORG' to the organic solvent phase, 'MeOH' to the methanol phase and 'PREC' to the precipitate after centrifugation of the respective extract.

2.2.1. Extraction with 0.1 M HCl in H_2O

Carbonates were removed by extracting 300 g of soil with 900 mL of a 0.1 M HCl solution for 3 h at 130 rpm. The soil extract was then centrifuged for 30 min and the supernatant filtered. A 20 mL aliquot of the filtrate was collected and freeze-dried for further analyses (AQU0). The soil residue was suspended in 600 mL of H_2O, shaken manually, and the supernatant discarded following centrifugation for 15 min. The soil residue (RES0) was then dried at 40 °C for 48 h and freeze-dried. For the subsequent Humeomics SCF, three replicates were taken from the freeze-dried soil residue (RES0).

2.2.2. Extraction with DCM/MeOH

The ORG1 fraction was obtained by extracting 40 g of RES0 with 120 mL of a DCM 2:1 MeOH (DCM/MeOH) solution (v/v) for 12 h at 130 rpm. The extracts were then centrifuged for 20 min and the supernatant filtered into a round-bottom flask. The extraction procedure was repeated but with 60 mL of solution for 1 h. The volume of the combined extracts was reduced to about 10 mL by rotary evaporation, and subsequently centrifuged at 12000 rpm (13870 *g*) for 20 min in order to separate the clay minerals (PREC1). The remaining supernatant (ORG1) was further rotary evaporated and dried under a N_2 gas flow. The soil residue (RES1) was then dried at 40 °C for 72 h.

2.2.3. Extraction with 12 % BF_3 in MeOH

In the next step, transesterification was carried out using a 12 % (1.9 M) BF_3 in MeOH solution. In this transesterification reaction, BF_3 serves as a Lewis acid catalyst. It catalyses the exchange of an organic group of an ester with the organic group of an alcohol, i.e. MeOH (McCarthy et al., 2020). The transesterification reaction mechanism on the example of triglyceride is illustrated in Fig. SI-1 in the supporting information.

30 g of RES1 was suspended in 40 mL solution of 12 % BF_3 in MeOH using Teflon tubes, and a constant temperature of 77 °C for 16 h using an oven. The extraction procedure was repeated twice but with 90 mL and 40 mL of solution for 12 h and 7 h, respectively. The combined extracts were then centrifuged for 20 min and the supernatant filtered into a round-bottom flask. The soil residue was suspended sequentially-five times in 30 mL of MeOH and shaken manually. Each extract was centrifuged for 20 min and the supernatant filtered into the round-bottom flask containing the BF_3 extract. Furthermore, the soil residue was resuspended again twice but in 20 mL of H_2O and shaken manually. Each extract was centrifuged for 20 min and the supernatant filtered into the round-bottom flask containing the BF_3 extract. This extract was then rotary-evaporated and transferred to a separation funnel, in order to obtain an organic phase (ORG2), a MeOH phase (MeOH2) and an aqueous phase (AQU2). This procedure involved adding a total of 110 mL of H_2O and 250 mL of chloroform to the separation funnel. The ORG2 fraction was dried with anhydrous sodium sulphate, filtered, rotary evaporated, and then dried under a N_2 gas flow. Similarly, the MeOH2 fraction was dried with anhydrous sodium sulfate following centrifugation for 20 min, filtered, rotary evaporated, and then dried under a N_2 gas flow. The precipitate after centrifugation was combined with the soil residue. The AQU2 fraction was filtered and then rotary evaporated. Replicates 1 and 2 of AQU2 were dialysed prior to freeze-drying by ultrafiltration with a 500 Da cut-off membrane against H_2O in order to remove ions, which could otherwise interfere with the analysis of C using GC–MS (not part of this paper). The water was changed twice a day until the electrical conductivity was below 1 μS/cm. Replicate 3 of AQU2 was directly freeze-dried for subsequent analysis of total P (P_{tot}). The soil residue (RES2) was then dried at 40 °C for 144 h.

The phosphate ester linkage of IP is considered to be quite stable with slow chemical hydrolysis in acidic media (Turner et al., 2002). Therefore, we assume that the transesterification process with BF_3 breaks mainly weak ester bonds between the SOM and organic molecules associated with the phosphate groups of IP, and not the ester bond between the phosphate groups and the inositol ring itself.

2.2.4. Extraction with 0.5 M KOH in MeOH

The soil residue RES2 was further fractionated by extracting 20 g with 30 mL of 0.5 M KOH in MeOH, which was stirred under a N_2 atmosphere and reflux at a constant temperature of 80 °C for 2 h. The soil residue was suspended sequentially-three times in acidified MeOH (pH = 2, using HCl) and shaken manually. Each extract was centrifuged for 20 min and the supernatant filtered and added to the KOH extract. Furthermore, the soil residue was washed again but with a non-acidified MeOH solution, and processed as previously described. The combined extracts were then centrifuged, filtered, rotary evaporated, and transferred to a separation funnel, in order to obtain an organic phase (ORG3), a MeOH phase (MeOH3) and an aqueous phase (AQU3). This involved adding a total of 250 mL of DCM, 20 mL of MeOH, and 80 mL of H_2O to the separation funnel. The ORG3, MeOH3, and AQU3 fractions were processed the same as that previously described. The soil residue (RES3) was then dried at 40 °C for 48 h.

2.2.5. Extraction with 47 % HI in H_2O

The last Humeomics SCF fraction was obtained by suspending 15 g of RES3 in a 20 mL solution of 47 % (11 M) HI in H_2O using Teflon tubes, and a constant temperature of 77 °C for 48 h using an oven. After cooling, the extract was centrifuged for 20 min and filtered into a plastic beaker. The soil residue was washed sequentially eleven times with 20 mL of H_2O for 30 min at 130 rpm. Each extract was centrifuged for 20 min and the supernatant filtered and added to the HI extract. However, approximately 200 mg of sodium carbonate was added to the eleventh H_2O extraction in order to increase the pH of the soil to above 5. Sodium carbonate was added stepwise under stirring to the soil extract in the plastic beaker until a pH of 7 was reached. The I_2 was neutralised with a stepwise addition of sodium thiosulfate-pentahydrate) until a colour change from reddish brown to grey-brown was observed. Replicates 1 and 2 of AQU4 were dialysed prior to freeze-drying as previously described. Replicate 3 of AQU4 was directly freeze-dried for subsequent analysis of P_{tot}. The soil residue (RES4) was then dried at 40 °C for at least 72 h.

2.3. Concentrations of total phosphorus in the untreated soil, in the SCF fractions and in the solid residues

Concentrations of P_{tot} in soil residues following each extraction step (UN, RES0, RES1, RES2, RES3, and RES4) were determined using microwave acid digestion. Briefly, 200 mg of ground soil was digested in 3 mL of a 65 % (14.4 M) NO_3 solution and 1 mL of a 37 % (12 M) HCl using a turboWAVE® MRT microwave digestion system (MILESTONE Srl, Sorisole, Italy) at 250 °C for 35 min (Fioroto et al., 2017). The digest was then made up to volume with H_2O and subsequently analysed for P using the malachite green method of Ohno and Zibilske (1991).

Concentrations of P_{tot} in the rotary evaporated fractions of the SCF were measured using the aforementioned microwave acid digestion method, except about 100 mg of dried material was digested in 2 mL of a 65 % NO_3 solution.

The proportion of P_{tot} extracted by the Humeomics SCF procedure ($P_{tot,H}$) in mg P/kg_{soil} to P_{tot} in the untreated soil ($P_{tot,UT}$) in mg P/kg_{soil} was calculated using equation Eq. (1):

$$P_{tot,H} : P_{tot,UT}\ (\%) = \frac{P_{ORG1} + P_{ORG2} + P_{ORG3} + P_{AQU0} + P_{AQU2} + P_{AQU3} + P_{AQU4} + P_{PREC1} + P_{MeOH2} + P_{MeOH3}}{P_{tot,\ UT}} * 100 \quad (1)$$

where P_{ORG1} to P_{MeOH3} are the P concentrations (mg P/kg_{soil}) in the respective dried SCF extracts. The concentrations were determined using microwave acid digestion with subsequent malachite green measurements of the diluted digests.

2.4. NaOH-EDTA extractable phosphorus in the untreated soil and in the solid residues

Concentrations of NaOH-EDTA extractable P in the untreated soil (UT) and soil residues following each extraction step (RES0, RES1, RES2, RES3, and RES4) were measured using the method of Cade-Menun et al. (2002). The soil was extracted with 0.25 M NaOH + 0.05 M EDTA at a 1:10 soil-to-solution ratio for 16 h at 150 rpm. Soil extracts were centrifuged for 15 min and filtered prior to analysis of P_{tot} by ICP-OES, and molybdate reactive P (MRP) by the malachite green method of Ohno and Zibilske (1991). The difference between P_{tot} and MRP is MUP, and considered to be largely that of organic P. An aliquot of all NaOH-EDTA filtrate for Replicate 3 was frozen at −80 °C and then freeze-dried for NMR analysis.

The proportion of $P_{tot,H}$ to P_{tot} measured in the NaOH-EDTA extract of the untreated soil ($P_{tot,UT,NE}$) in mg P/kg_{soil} was calculated based on equation Eq.1, but by replacing $P_{tot,UT}$ with $P_{tot,UT,NE}$.

2.5. Sample preparation for solution ^{31}P NMR spectroscopy

Sample preparation of freeze-dried material for solution ^{31}P NMR spectroscopy was similar to that reported in Reusser et al. (2020a). Briefly, 40 mg (UT, RES1, and RES2) or 80 mg (RES0, RES3, and RES4) of freeze-dried material was dissolved in 600 μL of NaOH-EDTA solution. The solution was then shaken and allowed to rest for at least 2 h, and then centrifuged at 10,000 rpm (10621 *g*) for 15 min. A 500 μL aliquot of the supernatant was transferred to a 1.5 mL microcentrifuge tube, which was then spiked with a 25 μL aliquot of 0.03 M methylenediphosphonic acid (MDP) standard in D_2O, and a 25 μL aliquot of sodium deuteroxide (NaOD) at 40 % (w/w) in D_2O. The solution was then transferred to a 5 mm NMR tube for analysis.

Sample preparation of the AQU0, AQU2, AQU3, and AQU4 freeze-dried materials was similar to that described above, except at a different material to solution ratio. The freeze-dried material of AQU0 was dissolved in 2 mL of NaOH-EDTA, and after centrifugation at 10,000 rpm (10621 *g*) for 15 min, a 600 μL aliquot of the supernatant was transferred to a 1.5 mL microcentrifuge tube and spiked with 25 μL of MDP in D_2O and 30 μL of NaOD. The freeze-dried material of AQU2 still contained moisture due to its high ion content. Briefly, a subsample of 40 mL was freeze-dried and dissolved in NaOH-EDTA to make a final volume of 12 mL. Several different dilution factors and additions of NaOD were tested but resulted in low-quality NMR spectra. Consequently, the concentrated ion solution was removed using ultrafiltration with a 1 kDa cut-off at 5000 rpm for 20 min. This resulted in an aliquot of 200 μL for the 1 kDa retentate, which was subsequently diluted with 550 μL of NaOD and centrifuged. A 500 μL aliquot was transferred to a 1.5 mL microcentrifuge tube and spiked with 25 μL of MDP, which then produced a high-quality NMR spectrum. The freeze-dried material of AQU3 (80 mg) and AQU4 (120 mg) was dissolved in 600 μL of NaOH-EDTA, and after centrifugation, a 500 μL aliquot of the supernatant was transferred to a 1.5 mL microcentrifuge tube and spiked with 25 μL of MDP and 30 μL of NaOD. All solutions were then transferred to a 5 mm NMR tube for analysis.

Sample preparation of the ORG1, ORG2, and ORG3 freeze-dried materials was similar to that described above, except 750 μL of deuterated chloroform ($CDCl_3$) was used as the dissolving agent. After centrifugation, a 500 μL aliquot was transferred to a 1.5 mL microcentrifuge tube and spiked with 25 μL of a 0.03 M triphenylphosphate (TPP) in $CDCl_3$. All solutions were then transferred to a 5 mm NMR tube for analysis.

2.6. Solution ^{31}P NMR spectroscopy and processing of spectra

Solution ^{31}P NMR analyses were carried in order to determine the P composition of the extracts and soil residues after each fractionation step. The ^{31}P NMR analyses were conducted at the NMR facility of the Laboratory of Inorganic Chemistry (Hönggerberg, ETH Zürich). All samples were analysed using a Bruker Avance III HD 500 MHz NMR spectrometer equipped with a 5 mm liquid-state Prodigy™ CryoProbe (Bruker Corporation; Billerica, MA). The ^{31}P frequency was set to 202.5 MHz with inverse gated broadband proton decoupling and 90° pulses (duration of 12 μs). The longitudinal relaxation time (T_1) of each sample was assessed in advance by an inversion recovery experiment. Detailed description of this experiment can be found in Reusser et al. (2020a). Recycle delays were then calculated by multiplying the longest T_1 value of the inversion recovery experiment times by 5 in order to achieve a full recovery (99.33 %) of point magnetisation (Claridge, 2016). This resulted in recycle delays ranging from 5 to 35 s for the NaOH-EDTA extracts and 5 to 14 s for the $CDCl_3$ extracts. An average of 4096 scans for each NMR spectrum was acquired for the NaOH-EDTA and $CDCl_3$ extracts.

Solution ^{31}P NMR spectra were Fourier transformed, phase corrected, and baseline adjusted using the TopSpin® software of Bruker (Version 4.1.0, Bruker Corporation; Billerica, MA). Line broadening was set to 0.6 Hz for all spectra. Quantification of NMR signal involved comparing the integral region of the added P standard (MDP or TPP) of known P concentration, with all other NMR signals which are directly relative to each other. Integral regions included: 1) phosphonates (δ 19.9 to 13.3 ppm), 2) the combined orthophosphate and phosphomonoester region (δ 6.2 to 2.9 ppm), 3) phosphodiesters (δ 2.8 to −2.0 ppm), 4) pyrophosphate (δ −4.8 to −5.5 ppm) and 4) polyphosphates (δ −17.1 to −20.6 ppm). Spectral deconvolution fitting was applied to the orthophosphate and phosphomonoester region due to overlapping NMR signals in this region, as described in Reusser et al. (2020a). Peak assignments were based on spiking the extracts with standard solutions of the respective P_{org} compound and comparing the chemical shift with reported values of known compounds (Cade-Menun, 2015; Doolette et al., 2009; Reusser et al., 2020b).

The proportion of a specific P compound removed by the Humeomics SCF from the soil residue ($P_{removed}$) was assessed using equation Eq. (2):

$$P_{removed}\,(\%) = \frac{P\,conc.\ RES_x - P\,conc.\ RES_{x+1}}{P\,conc.\ RES_x} * 100 \quad (2)$$

where 'P conc. RES_x' is the concentration of the respective P compound (mg P/kg_{soil}) determined by NMR in the NaOH-EDTA extract of the soil residue before the Humeomics SCF extraction step (RES_x), and 'P conc. RES_{x+1}' is the concentration of the respective P compound (mg P/kg_{soil}) in the soil residue after the Humeomics SCF extraction step (RES_{x+1}).

2.7. Concentrations of total carbon and total nitrogen in the untreated soil and in the solid residues

Concentrations of total C and total N in the soil residues following each extraction step (RES0, RES1, RES2, RES3, and RES4) were determined using dry combustion (vario PYRO cube®, Elementar Analysesysteme GmbH). About 5 mg of soil was weighed into tin foil capsules, which were then placed into the C and N analyser and subsequently combusted at 950 °C.

2.8. Solid-state CPMAS ^{13}C NMR spectroscopy

All solid-state cross polarisation magic angle spinning (CPMAS) ^{13}C NMR analyses were carried out at the Interdepartmental Research Centre on NMR for the Environment, Agro-food and New Materials (CERMANU) of the University of Naples Federico II in Portici, Italy. All samples were analysed using a Bruker Avance 300 MHz wide-bore NMR

Table 1
Concentrations of total P (P_{tot}) as measured by HNO_3-HCl microwave digestion; P_{tot}, organic P (P_{org}) and inorganic P (P_{inorg}) in 0.25 M NaOH + 0.05 M EDTA extracts; total C (C_{tot}) and total N (N_{tot}) as measured by combustion. Standard deviations of n = 3 replicates are shown in brackets, with the solely analytical replicates marked with an asterisk.

Measure	UT	RES0	RES1	RES2	RES3	RES4
P_{tot} digestion	1796(43)	1579(28)	1561	995	934	437
(mg P/kg_{soil})	*	*	(33)	(105)	(40)	(60)
P_{tot} NaOH-EDTA extract (mg P/kg_{soil})	1682	1518	1555	648	661	621
	-	-	(44)	(35)	(80)	(14)
P_{org} NaOH-EDTA extract (mg P/kg_{soil})	972	829	865	450	450	462
	-	-	(50)	(24)	(53)	(5)
P_{inorg} NaOH-EDTA extract (mg P/kg_{soil})	709	689	690	199	211	160
	-	-	(10)	(19)	(28)	(9)
C_{tot} (g C/kg_{soil})	159(0.4)	134(0.9)	131	73	70	80
	*	*	(0.6)	(3.9)	(1.6)	(0.9)
N_{tot} (g N/kg_{soil})	11(0.1)	9(0.1)	10	5	5	3
	*	*	(0.1)	(0.4)	(0.1)	(0.2)
C_{tot}: N_{tot}	14	15	13	15	14	27
C_{tot}: P_{org}	163	162	149	172	151	175

spectrometer equipped with a CPMAS probe. Soil was packed into a 4 mm Zirconia rotor fitted with Kel-F end-caps, which was spun at 13000 Hz. The ^{13}C frequency was set to 75.47 MHz and spectra were obtained using a ramped-amplitude CP pulse sequence, in which the ^{1}H spin lock power was varied linearly during the contact time (Mazzei and Piccolo, 2015). Each NMR spectrum was acquired using a 1 ms contact time, a recycle delay of 2 s, and an average of 32,000 scans.

Solid-state ^{13}C NMR spectra were Fourier transformed, phase corrected, and baseline adjusted using the TopSpin® software of Bruker (Version 4.1.0, Bruker Corporation; Billerica, MA). Line broadening was set to 200 Hz for all spectra. Integral regions were measured and peak assignments were carried out according to Stevenson (1994) and Spaccini et al. (2006). This included: 1) 0–50 ppm, alkyl-C (e.g. alkanes and fatty acids); 2) 50–85 ppm, C—O and C—N in ethers, esters, carbohydrates and amines (e.g. amino acid-peptide- and protein-C); 3) 85–105 ppm, aliphatic C—O (carbohydrates); 4) 105–160 ppm, aromatic C with phenolic C between 150–160 ppm, and; 5) 160–200 ppm carbonyl-C. Integral regions 1) and 4) are considered to represent mostly hydrophobic compounds, whereas those of 2), 3), and 5) are considered mostly to comprise of hydrophilic compounds (Spaccini et al., 2006). Furthermore, the alkyl-C region of 1) can also be referred to the aliphatic region, whereas regions 2) and 3) are also known as the *O*-alkyl region (Simpson and Simpson, 2017).

2.9. Statistical analyses and graphics

After the HCl extraction, the soil sample was divided into three replicates. The further SCF extraction steps were carried out on each replicate independently. The UT soil and RES0 were divided into three analytical replicates for the analyses. For the other soil residues RES1-RES4, the calculations of the averages and standard deviations are based on the 'true' replicates of the SCF. Solid-state CPMAS ^{13}C NMR, solution ^{31}P NMR spectroscopy and P_{tot} measurements of the dried SCF extracts were only carried out on one SCF replicate (replicate 3).

Calculations of replicate averages, standard deviations and correlation coefficients were carried out using Microsoft® Excel 2016. One-way ANOVA with subsequent multi-comparison of mean values were processed in MATLAB R2017a (©The MathWorks, Inc.). The multi-comparison of means calculation was based on the Tukey's honestly significant difference procedure using the Studentised range distribution (Hochberg and Tamhane, 1987; Milliken and Johnson, 2009). All graphics of solution ^{31}P NMR spectra were created in MATLAB R2017a. All solution ^{31}P NMR spectra were normalised to the peak maximum of the MDP peak. All other graphics, including solid-state ^{13}C NMR spectra, were created in Microsoft® Excel 2016.

3. Results

3.1. Carbon

3.1.1. Concentrations of total carbon in Humeomics residues

The removal of carbonates with 0.1 M HCl caused a significant decrease in total soil C (C_{tot}) of 24 g C/kg_{soil} (15 % of 159 g C/kg_{soil} in the UT soil) (Table 1, Fig. SI-2). Following this, the Humeomics SCF procedure extracted on average 64 g C/kg_{soil}, corresponding to 40 % of C_{tot} in the UT soil. The majority of C_{tot} (58 g C/kg_{soil}) was removed by the BF_3 in MeOH extraction. No significant differences in C_{tot} were found between RES0 and RES1 (DCM/MeOH extraction) and between RES2 and RES3 (0.5 M KOH in MeOH extraction). There was a significant increase in C_{tot} of 10 g C/kg_{soil} from RES3 to RES4, following the 47 % HI in H_2O extraction step and subsequent neutralisation of soil acidity using sodium carbonate. Approximately 200 mg sodium carbonate were added to 20 g of soil in this neutralisation step, which calculates to an input of 1.2 g C/kg_{soil} to RES 4.

3.1.2. Chemical nature of carbon in soil Humeomics residues

The chemical nature of C in the UT soil and soil residues following each step of the SCF procedure was assessed by solid-state CPMAS ^{13}C NMR spectroscopy (Fig. 2). There was no difference in the chemical nature of C in the UT soil and the soil residue following 0.1 M HCl treatment (RES0). However, NMR signals in the alkyl-C region slightly decreased following the DCM/MeOH treatment (RES1) compared to RES0. Most notably, there was a large decrease of NMR signals in the alkyl-C region and the region representing C—O and C—N bonds in ethers, esters, carbohydrates and amines following the 12 % BF_3 in MeOH treatment (RES2) compared to RES1. The 12 % BF_3 in MeOH treatment also revealed the presence of a peak (δ 50–60 ppm), which was assigned to *N*-alkyl and methoxyl-C (Stevenson, 1994). Furthermore, the 12 % BF_3 in MeOH treatment also removed some carbonyl-C (region 5) and aliphatic C—O (region 3), and *N*-alkyl, methoxyl-C and aliphatic C—O (region 2). The 0.5 M KOH in MeOH treatment resulted in a large decrease of NMR signals in the aliphatic C—O and *N*-alkyl, methoxyl C and aliphatic C—O regions of RES3 compared to RES2. The chemical nature of C in RES4 was largely hydrophobic alkyl-C (region 1) and aromatic C (region 4) following 47 % HI in H_2O.

[Suggested location Fig. 2].

3.2. Phosphorus

3.2.1. Concentrations of total phosphorus in Humeomics extracts

The Humeomics SCF procedure extracted a total of 1158 mg P/kg_{soil}

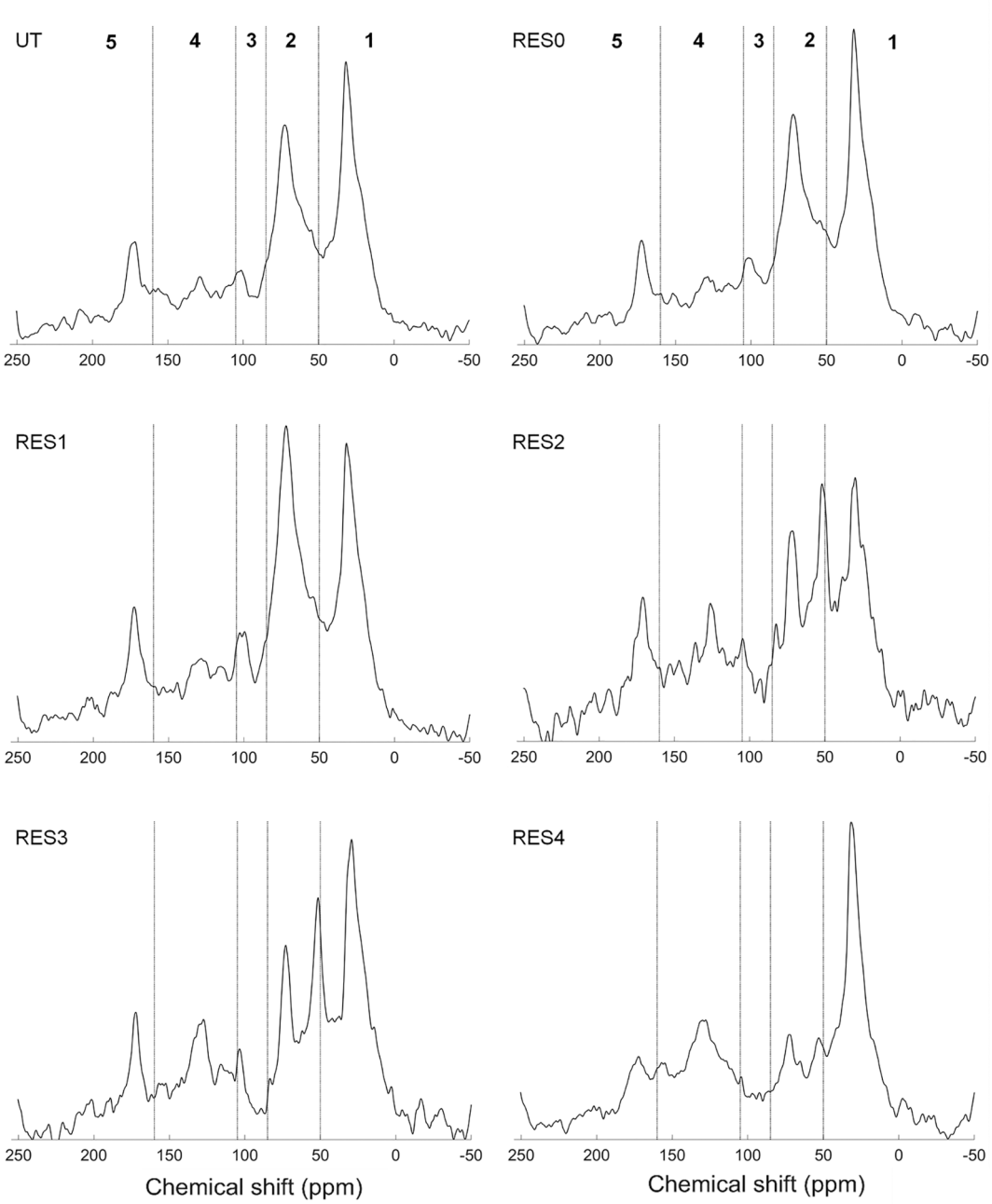

Fig. 2. Solid-state ^{13}C cross polarisation magic angle spinning (CPMAS) NMR spectra on the untreated soil (UT) and the soil residues (RES0, RES1, RES2, RES3, and RES4) after each step of the Humeomics sequential chemical fractionation procedure. Chemical shift ranges of different C species are separated by dotted lines and labelled with numbers: alkyl-C (1), C–O and C–N in ethers, esters, carbohydrates and amines (2), aliphatic C–O as in carbohydrates (3), aromatic C (4) and carbonyl C (5).

(Table SI-1 in the supporting information, sum of P_{tot} measured in the digests of the dried extracts), which accounted for 64 % of P_{tot} in the Gleysol, as determined by microwave acid digestion (Table 1). Concentrations of P_{tot} in each of the Humeomics extracts were low, except for the 47 % HI in H_2O extract (AQU4), which was 1040 mg P/kg_{soil} and comprised 90 % of extractable P by Humeomics (Table SI-1 in the supporting information). Negligible concentrations of P were present in the organic phases of Humeomics extracts.

3.2.2. Chemical nature of phosphorus in Humeomics extracts

Solution ^{31}P NMR spectroscopy revealed that the majority of P in Humeomics extracts occurred as orthophosphate in the aqueous phases of the 12 % BF_3 in MeOH (AQU2) and 47 % HI in H_2O (AQU4) extracts (Table SI-1 and Fig. SI-3), which comprised more than 90 % of extractable P by Humeomics. In general, phosphomonoesters were the dominant pool of organic P in Humeomics extracts, particularly in the aqueous phases of 0.5 M HCl (AQU0) and 47 % HI in H_2O (AQU4) extracts, albeit at low concentrations (<5 mg P/kg_{soil}). Several sharp (and broad) unidentified signals were present in the phosphomonoester region across all aqueous phases.

3.2.3. Concentrations of phosphorus pools in Humeomics residues

In total, 1359 mg P/kg_{soil} of P_{tot} in soil was removed by the SCF procedure, resulting in 76 % of P_{tot} in UT (1796 mg P/kg_{soil}, Table 1). Most P was extracted by the 12 % BF_3 solution, leading to a decrease of the P_{tot} concentrations in the soil residues of 566 mg P/kg_{soil} (36 % of

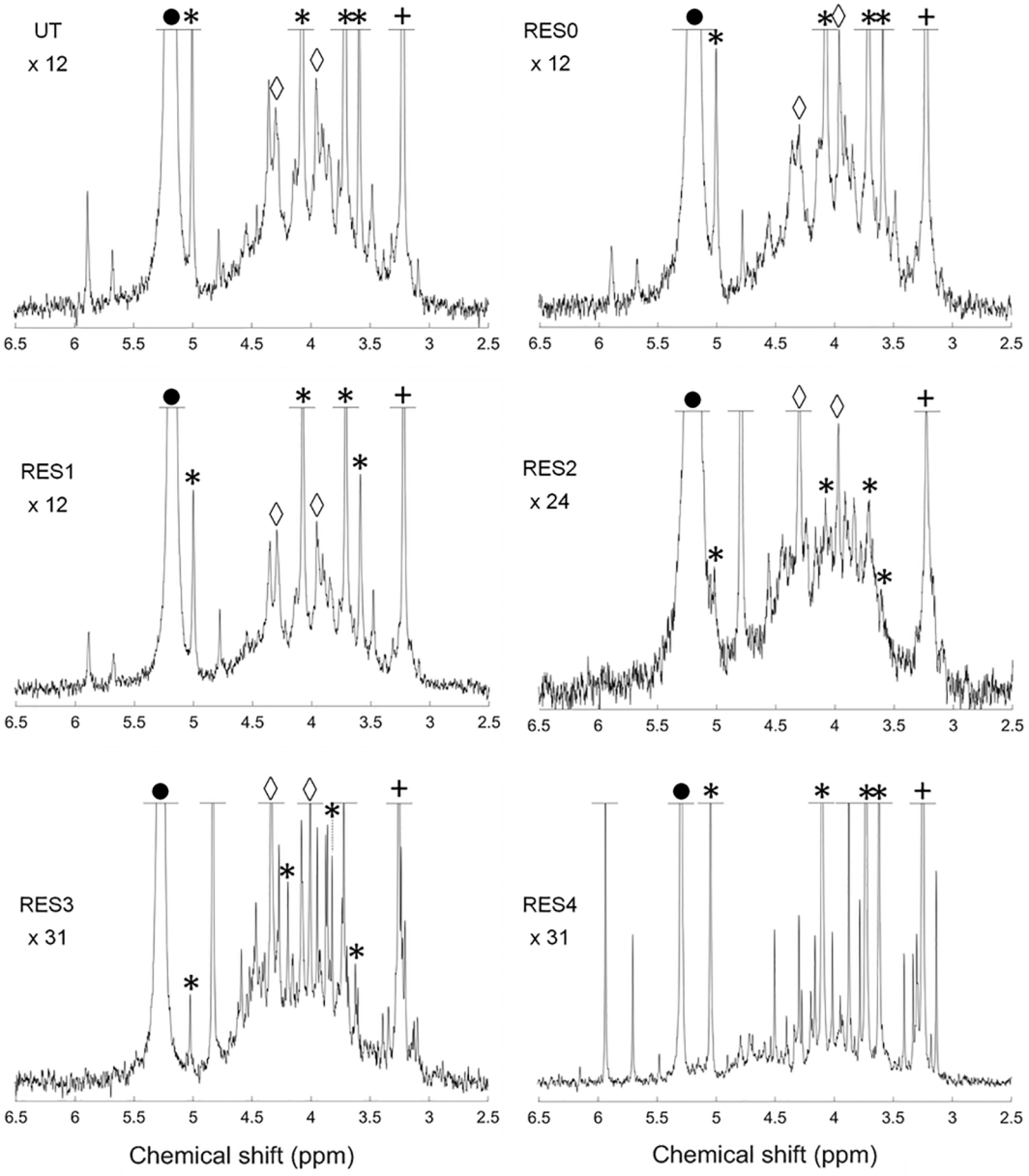

Fig. 3. Solution ^{31}P NMR spectra (500 MHz) of the orthophosphate and phosphomonoester region on 0.25 M NaOH + 0.05 M EDTA Humeomics soil residues extracts. Signal intensities were normalised to the MDP peak intensity. The vertical axes were increased for improved visibility of spectral features, as indicated by a factor. The asterisk marks the four individual peaks of *myo*-IP$_6$, the '+' the peak of *scyllo*-IP$_6$, the '●' the orthophosphate peak and the symbol '◊' the two peaks of α- and β-glycerophosphate.

P_{tot} in RES1). Another significant pool of P (on average 497 mg P/kg$_{soil}$) was removed by the 47 % HI extraction. In contrast, the other Humeomics extraction steps did not decrease the P_{tot} contents in the soil residues in a significant amount except for the HCl extractable P (Fig. SI-5). The remaining soil residue RES4 contained 437 mg P/kg$_{soil}$ (Table 1), corresponding to 24 % of P_{tot} in UT.

Similar to the P_{tot} results, the 12 % BF_3 extraction led to a significant decrease of the NaOH-EDTA extractable P pool of 907 mg P/kg$_{soil}$ (58 % of P_{tot} NaOH-EDTA in RES1, Table 1, Fig. SI-6). This decrease was more pronounced for P_{inorg}, with a reduction of 71 % (on average 491 mg P/kg$_{soil}$), compared to P_{org}, with a reduction of 48 % (on average 415 mg P/kg$_{soil}$). Consequently, the proportion of P_{org} to total NaOH-EDTA extractable P increased from 58 % in UT to 74 % in RES4 after the Humeomics sequential extraction method. In addition, slightly more P_{org} was extracted in RES4 compared to RES3. The final soil residue RES4 contained on average 621 mg P/kg$_{soil}$ NaOH-EDTA extractable P_{tot} (Table 1, replicate 3: 611 mg P/kg$_{soil}$ NaOH-EDTA extractable P_{tot}).

Not all of P_{tot} removed in the Humeomics residues was recovered in the extracts. This was mostly the case for the 12 % BF_3 extraction, where the NaOH-EDTA extractable P_{tot} in the soil residues decreased by 907 mg P/kg$_{soil}$, but only 99 mg P/kg$_{soil}$ were measured by microwave digestion in the respective dried extracts combined.

3.2.4. *Chemical nature of phosphorus in soil Humeomics residues*

The chemical nature of P in the UT soil and soil residues following each step of the Humeomics SCF procedure was assessed by solution ^{31}P NMR spectroscopy on NaOH-EDTA extracts (Fig. 3). The whole spectra of UT and RES4 as well as a detailed peak assignment in the combined phosphomonoester and orthophosphate region can be found in Figs. SI-7. SI-8 and SI-9 in the supporting information.

In general, most P was detected in the combined *ortho*-P + phosphomonoester region, followed by phosphodiesters and pyrophosphates

Table 2
Concentrations (mg P/kg_{soil}) of phosphonates, orthophosphate (*ortho*-P), the sum of all inositol phosphates (inositol-P) with a detailed list of all identified IP isomers below, α- and β-glycerophosphate (glycerol-P), broad peaks, other phosphomonoester (P-monoester), phosphodiester (P-diester), pyrophosphates (pyro-P), polyphosphates (poly-P) and total P (P_{tot}) measured in solution ^{31}P NMR spectra of 0.25 M NaOH + 0.05 M EDTA soil residues of the Humeomics fractionation procedure. Quantification was based on spectral integration, deconvolution fitting and the relative proportion to the peak of the added MDP standard of known concentration.

P-class	UT	RES0	RES1	RES2	RES3	RES4
Phosphonates	2	3	2	2	2	1
Ortho-P	642	630	597	173	164	100
Total Inositol-P	312	229	275	35	40	212
myo-IP_6	159	119	139	11	10	93
scyllo-IP_6	70	58	57	20	12	54
neo-IP_6	38	31	27	0	0	13
D-*chiro*-IP_6	26	10	37	0	0	15
myo-(1,2,4,5,6)-IP_5	12	8	8	0	9	22
scyllo-IP_5	7	5	7	4	10	14
***Glycero*-P**	33	35	20	19	21	0
Broad peaks	272	263	211	138	102	83
Glucose-6-P	4	4	5	20	21	0
Other P-monoester	39	32	48	26	38	76
P-diester	49	51	65	13	13	1
Pyro-P	43	37	38	0	1	0
Poly-P	4	0	0	0	0	0
P_{tot} NMR	1400	1283	1262	427	402	473

(Table 2). Phosphonates and polyphosphates were only measured in trace amounts. The phosphomonoester region comprised of three main spectral features, including a dominant *ortho*-P peak, two to three underlying broad signals, and on average 31 sharp peaks. The 0.5 M KOH in MeOH extraction resulted in an increase of detectable sharp peaks in the phosphomonoester region of the soil residues, i.e. from 24 sharp peaks in RES2 to 39 resp. 40 in RES3 resp. RES4. The distribution of specific P compounds along the Humeomics fractions are presented in the following sections in more detail.

Untreated soil

The majority of P in UT was present in the form of orthophosphate (642 mg P/kg_{soil}, 46 % of P_{tot} NMR), inositol phosphates (312 mg P/kg_{soil}, 22 % of P_{tot} NMR) and one underlying broad signal in the phosphomonoester region representing the unresolved P_{org} pool (272 mg P/kg_{soil}, 19 % of P_{tot} NMR). The remaining 13 % of P_{tot} as measured by NMR included forms of phosphodiesters, other phosphomonoesters, pyrophosphates, polyphosphates and phosphonates.

The most abundant form of IP was the *myo*-isomer of IP_6 (51 % of total IP). Two inositol pentakisphosphates *myo*-(1,2,4,5,6)-IP_5 and *scyllo*-IP_5 were also detected.

0.1 M HCl in H_2O extraction

The extraction with 0.1 M HCl did not cause a considerable change of the P composition in the NMR spectrum on the soil residue RES0. However, regarding concentrations, 9 mg P/kg_{soil} (3 %) of the unresolved P_{org} pool and 83 mg P/kg_{soil} (27 %) of the total IP pool were apparently removed by the 0.1 M HCl extraction.

DCM/MeOH extraction

Similar to the previous extraction step, the organic solvent extraction did not cause a considerable change in P composition, except that 52 mg P/kg_{soil} (20 %) of the unresolved P_{org} pool was removed. Because of this reduction, the remaining unresolved P_{org} pool was represented by two underlying broad signals in the phosphomonoester region of RES 1. In contrast to this pool, the organic solvent extraction resulted in a higher NaOH-EDTA extractability of IP and phosphodiesters in RES1.

% BF_3 in MeOH extraction

The 12 % BF_3 extraction did not only remove most of P from the soil, but also markedly changed the molecular composition of the remaining P pool in the residue RES2. Compared to RES1, 424 mg P/kg_{soil} (71 %) of orthophosphate, 73 mg P/kg_{soil} (35 %) of the unresolved P_{org} pool, 240 mg P/kg_{soil} (87 %) of IP, and 52 mg P/kg_{soil} (80 %) of phosphodiesters were removed by the 12 % BF_3 extractant. Furthermore, pyrophosphates were completely removed.

This extraction step gave rise to a sharp peak at δ 4.79 ppm, which was attributed to glucose-6-phosphate based on spiking the AQU3 extract with a standard solution. Contrasting to all other P compounds, the concentration of glucose-6-phosphate increased markedly (4-times) in the NaOH-EDTA extract of RES2 compared to RES1.

0.5 M KOH in MeOH extraction

The subsequent 0.5 M KOH extraction caused again a decrease of 36 mg P/kg_{soil} (26 %) of the unresolved P_{org} pool represented by one underlying broad signal in the phosphomonoester region of RES3. However, the extraction did not much affect *myo*-IP_6 but decreased the *scyllo*-IP_6 concentration by 8 mg P/kg_{soil} (40 %) compared to RES2. This decrease was in line with the reappearance of *myo*-(1,2,4,5,6)-IP_5 and a major increase of *scyllo*-IP_5 by 6 mg P/kg_{soil} (250 %) in the NaOH-EDTA extract of RES3.

47 % HI in H_2O extraction and residual fraction

Only 83 mg P/kg_{soil} (31 %) of the unresolved P_{org} pool represented by underlying broad signals in solution ^{31}P NMR spectra was left in the residual soil RES4 of the Humeomics SCF procedure compared to UT. This unresolved P_{org} pool was represented by two underlying broad signals in the phosphomonoester region of the NMR extract on the residual fraction.

The last Humeomics extraction step caused a large increase of the NaOH-EDTA extractable IP pool. All four isomers of IP_6 were again detected in the last residue. In summary, an additional pool of 172 mg P/kg_{soil} IP could be extracted compared to RES3, with the total IP pool in RES4 comprising 45 % of P_{tot} analysed by NMR. The dominance of IP in the residual soil after the Humeomics SCF can also be seen in the NMR spectra of RES4 in Fig. 3. A plethora of sharp peaks in the phosphomonoester region were detected (40), half of them were assigned to different IP isomers and conformations. It was possible to distinguish the peaks of the 2-equatorial-4-axial and 4-equatorial-2-axial conformation of D-*chiro*-IP_6 as well as the ones of the 2-equatorial-4-axial and 4-equatorial-2-axial conformations of *neo*-IP_6 (Figure SI-9). All increases in the NaOH-EDTA extractable IP add up to 223 mg P/kg_{soil}. Therefore, at least 71 % more IP could be extracted by Humeomics compared to a single-step NaOH-EDTA extraction (UT).

Phosphodiesters were almost completely removed following the Humeomics SCF. Two pools of phosphodiesters can be distinguished: one extracted with 12 % BF_3 (52 mg P/kg_{soil}) and one extracted with 47 % HI (12 mg P/kg_{soil}).

4. Discussion

4.1. Carbon content and speciation in different SOM fractions

About half of the C present in the soil was removed by the Humeomics SCF procedure. Similar to our findings, Drosos et al. (2017) found that the organo- and hydrosoluble fractions of the 12 % BF_3 transesterification process contained most of the extracted C of an agricultural sandy loam soil classified as Typic Ustifluvent (Piccolo, 2012). The authors reported intense *O*-alkyl signals and high abundance of fatty acids and sugars with minor amounts of phenolic acids, imines, esters, dicarboxylic acids and hydroxyacids in the ORG2 fraction. Equally to ORG2, the AQU2 fraction of their study showed intense signals in the *O*-alkyl region indicating an abundance of hydroxyl- and methoxyl-rich molecules and minor amounts of alkyl-C and aromatic-C (Drosos et al., 2017). The ^{13}C CPMAS NMR results on the soil residues of this study indicate that mostly *O*-alkyl rich compounds as carbohydrates but also alkyl-C rich compounds were extracted by cleavage of weak ester bonds. Furthermore, methoxyl-C compounds appear to be less abundant in the ORG2 + AQU2 fraction compared to the results of Drosos et al. (2017) because of their enrichment in RES2.

Interestingly, the Gleysol did not contain significant amounts of

unbound C. Our results indicate that most organic molecules present in the Gleysol of this study are either part of a larger association/bound to the mineral phase or are rapidly biodegraded/incorporated when unbound. Furthermore, strong ester bonds and ether bonds appear to be rather irrelevant for the assembling of organic molecules in the SOM suprastructure of our soil. These results are in agreement with Nebbioso and Piccolo (2011), who found that only 0.9 % of the original humic acid weight was extracted with the strongly-bound fraction. The organo-soluble and hydrosoluble molecules after methanolic hydrolysis (strongly-bound ester fraction) accounted for 2.4 % of total SOM solubilised by Humeomics (Drosos et al., 2017). An explanation for the negligible effect of the KOH in MeOH extraction could be that the released OH-ions react with the soil buffer system, e.g. exchangeable Al^{3+} (Blume et al., 2009), before reacting with the SOM, hence reducing the catalysis capacity for the methanolic hydrolysis. The pH of the Gleysol soil sample used in this study was 5.0, measured in H_2O (Reusser et al., 2020a).

The soil residue after the Humeomics procedure still contained 80 g C/kg_{soil} C. However, there was a slight increase in C_{tot} from RES3 to RES4, possibly due to the addition of sodium carbonate to the soil residue in order to increase the pH or due to residues of MeOH. Drosos et al. (2017) reported that 37.4 % of total soil organic C was left in the residue after the Humeomics fractionation procedure (corresponding to RES3). The SOM in this pool is assumed to be closely associated to the soil mineral matrix and consist of alkyl structures (Drosos et al., 2017; Spaccini et al., 2006). These hydrophobic components are thought to be of great importance in the stabilisation of SOM due to the entropy driven repulsion and hence separation from the watery soil solution (Spaccini et al., 2006) and adsorption to aluminosilicate surfaces (Drosos et al., 2017; Kleber et al., 2007). The general increase of the relative amount of alkyl-C during biodegradation as part of the 'persistent' SOM is well known (Kögel-Knabner, 1997; Simpson and Simpson, 2017). Kögel-Knabner et al. (1992) found an accumulation of rigid alkyl-C moieties in forest SOM but attributed it to an increase in cross-linking during the humification process. Hence, our findings on the dominance of hydrophobic alkyl-C and aromatic-C in the non-extracted SOM pool agree well with previous studies on the 'persistent' SOM pool.

4.2. Extractability of P using the Humeomics SCF procedure of SOM

Overall, the Humeomics sequential fractionation procedure with subsequent NaOH-EDTA extraction of the final soil residue recovered similar amounts of P_{tot} when compared to a single-step NaOH-EDTA extraction of the UT soil.

Analysis of the different extracts and residues revealed that 66 % of P_{tot} was extracted using the 12 %BF_3 in MeOH solution, which is attributed to the fraction associated with the SOM suprastructure through weak ester bonds (Nebbioso and Piccolo, 2011). However, not all of the extracted P was recovered in the extracts, most likely due to losses in the preparation process of the extracts for total microwave digestion. Especially AQU2 was difficult to freeze-dry and quantitatively measure due to the high ion content. Only removal of the < 1 kDa fraction allowed for solution ^{31}P NMR spectroscopic analysis, which revealed that 279 mg P/kg_{soil} was present in the AQU2 extract. Therefore, we assume that concentrations of P_{tot} especially in the AQU2 extract are underestimated and quantitative evaluation of the extractability of P compounds using Humeomics should rather be based on the differences in the soil residues in this study.

Interestingly, more P_{tot} could be extracted from the final residue RES4 with NaOH-EDTA compared to the acid digestion. This would indicate that the remaining P compounds in RES4, which are assumed to be closely associated with the soil mineral phase, appear to be more prone to the alkaline oxidation and hydrolysis with NaOH compared to the harsh acidic hydrolysis of the digestion. However, this needs to be tested on different soil samples.

4.3. Extraction of phosphorus species with SOM fractions

The findings of this study suggest that not only the total content of P associated with SOM varies between SOM pools but also the composition of P. So far, most studies on soil C to P ratios focus on total P_{org} concentrations and do not investigate the P_{org} composition (Goh and Williams, 1982; John et al., 1965; Neptune et al., 1975; Stevenson, 1986). The average C:P_{org} ratio in this study was 162 and therefore in range of SOM ratios reported by various studies (Goh and Williams, 1982; Stevenson, 1986; Tipping et al., 2016). Our findings further reveal that the SOM structure is enriched in various P_{org} compounds such as IP, the unresolved P_{org} pool, other phosphomonoesters and phosphodiesters, whereas the SOM pool associated with the mineral phase is clearly enriched in IP compared to other P compounds.

4.3.1. Unresolved P_{org} pool

Our results provide further evidence that the unresolved P_{org} pool is not comprised of a single, large polymeric structure with C—C bonds and phosphate as functional groups as previously hypothesised (McLaren et al., 2015). In this study, subsequent cleavage of the SOM associations without breaking any C—C bonds led to a decrease of the unresolved P_{org} pool. The associations of the unresolved phosphomonoesters with other organic molecules of the SOM would result in the apparent high molecular size reported by Jarosch et al. (2015); McLaren et al. (2015) and McLaren et al. (2019). The phosphate containing molecules causing the broad signals are mostly associated with the SOM through weak and strong ester linkages (40 %) as defined by Nebbioso and Piccolo (2011). This close association with the SOM structure could result in the described resistance of the unresolved P_{org} pool to enzymatic hydrolysis (Jarosch et al., 2015) and chemical stability (Reusser et al., 2020b), because the accessibility is limited due to the hydrophobic nature and complex structure of these associations, possibly hindering microbial attack (Schmidt et al., 2011).

A smaller proportion of the unresolved phosphomonoesters (unbound fraction) appear to be free or part of associations held together only by weak dispersive forces (22 %). Another part (30 %) is still present in the SOM pool associated with the soil mineral phase. It is not known whether this remaining unresolved P_{org} pool exhibits a polymeric structure or not. Drosos et al. (2017) reported that the SOM fraction associated with the mineral phase consisted of mostly oxygen and nitrogen heterocyclic compounds, benzoic acids, and esters. Drosos et al. (2017) proposed that in this fraction, alkyl apolar components assemble by hydrophobic dispersive forces into larger size aggregates. These findings would suggest that the unresolved pool of P_{org} is not of a macropolymeric structure.

McLaren et al. (2019) and Reusser et al. (2020b) found based on transverse relaxation experiments that the underlying broad peaks in the phosphomonoester region were not caused by a series of IP species due to differences in their transverse relaxation times. This study provides further evidence that the broad peaks represent several components of unresolved phosphomonoesters, as the extractability trend of these compounds by subsequent extraction of the SOM structure was different compared to the extractability trend of the IP and other phosphomonoesters of known chemical nature.

4.3.2. Inositol phosphates

Two major pools of IP have been identified: the first pool being closely associated with the SOM and the second pool with the soil mineral phase. The association of IP with the SOM suprastructure would explain the occurrence of IP in high molecular weight organic compounds (Borie et al., 1989; Moyer and Thomas, 1970; Veinot and Thomas, 1972).

The extractability of IP could be markedly enhanced using the Humeomics SCF with results indicating that only 58 % of the total IP pool in soil can be extracted using a single-step NaOH-EDTA extraction. Furthermore, we assume that many sharp peaks in the

phosphomonoester region of RES4 could be attributed to unknown IP based on a hypobromite oxidation study on the same soil (Reusser et al., 2020b), resulting in an even higher total IP pool in the investigated soil. Previous studies on quantitative analysis of IP using NMR were mostly based on a single alkaline extraction step (McLaren et al., 2019; Reusser et al., 2020a; Turner et al., 2003; Turner and Richardson, 2004).

The enhanced extractability of IP could be due to the sequential 'decoating' of the SOM suprastructure by the SCF and the resulting enhanced accessibility of P compounds for the NaOH-EDTA extractant. Especially hydrophobic compounds separating the SOM suprastructure from the soil solution were removed by the DCM/MeOH extraction (Nebbioso et al., 2015; Spaccini et al., 2006), possibly leading to better extractability of incorporated P by the aqueous NaOH-EDTA solution. However, these findings need to be verified in further studies using different soil types.

Drosos et al. (2017) suggested that stabilisation of the SOM pool associated with the mineral phase should also be attributed to complex formation between oxygen-containing hydrophilic groups and iron minerals. The phosphate groups of IP would fulfil these requirements and serve as important bonding molecules between the soil mineral phase and SOM. Furthermore, IP are well known for their adsorption affinity to minerals and organic matter (Cosgrove and Irving, 1980; Ognalaga et al., 1994). Hence, the high abundance of IP in the final residue could be due to IP released from the soil mineral phase through acidic hydrolysis of oxides by HI.

Tipping et al. (2016) reported that according to their mixing-model P contributes 3 % to the total mass of 'nutrient rich' SOM, which describes the SOM fraction stabilised by sorption to the mineral phase. Frossard et al. (2016) as well as Tipping et al. (2016) proposed that specific molecules such as *myo*-IP_6 are possibly selectively incorporated into this SOM pool because of their strong sorption capacity. Our findings on the final residue after the Humeomics SCF are in agreement with the suggestion of Tipping et al. (2016) that *myo*-IP_6 is the most prevalent form in the SOM fraction associated with the mineral phase.

The significant reduction of IP in the transesterification process with BF_3 is assumed to result mainly from breaking weak ester bonds between the SOM and organic molecules associated with the phosphate groups. However, no IP has been recovered in the AQU2 fraction. Therefore, we suggest to test the effect of the BF_3 catalysed transesterification on pure IP standards as well as on soils containing a known concentration of IP.

4.3.3. Other P species

Glycerophosphates are hydrolysis products of phospholipids e.g. phosphatidylcholine (Doolette et al., 2009) as part of cell membranes (Strickland, 1973). Therefore, we can assume that the original phospholipids in the investigated soil were either unbound, part of the microbial biomass or completely liberated by breaking the ether bonds of the SOM structure through acidic hydrolysis. The removal of phospholipids in the unbound fraction appears to be coupled with the removal of alkyl-C as in fatty acids (Stevenson, 1994). However, the observed removal of phospholipids in the last residue was not coupled with a decrease in alkyl-C.

Further research is needed to investigate the formation and transformation processes of these P-SOM associations in soils of diverse SOM and P_{org} composition. Furthermore, the effects of the Humeomics SCF steps on standard P_{org} compounds should be tested in order to rule out any extraction artefacts. Especially the transesterification process catalysed by BF_3 needs further investigation. The large amount of orthophosphate with the concomitant absence of P_{org} compounds in AQU2 could indicate that the P_{org} compounds themselves were transesterified, i.e. the bond between the phosphate group and the organic molecule being broken. The proportion of P_{org} compounds destroyed by the BF_3 extraction needs to be evaluated in order to assess the proportion of P_{org} actually liberated from the SOM suprastructure.

5. Conclusions

The combination of the Humeomics SOM fractionation procedure with solution ^{31}P NMR spectroscopy revealed that the most abundant form of P_{org} in the soil, the unresolved phosphomonoester pool, is closely associated with the SOM suprastructure. The decrease of the unresolved phosphomonoesters with subsequent fractionation of the SOM structure advances our understanding of its chemical nature away from the macropolymeric theory and more towards an association point of view. Our study provides new insight on the chemical nature of the unresolved phosphomonoesters and how they are associated within the SOM structure. Furthermore, our findings indicate that especially the pool of IP in soil is underestimated using a single-step NaOH-EDTA extraction for soil P_{org} determination. These relatively stable P_{org} compounds dominated the residual fraction of the Humeomics SOM fractionation procedure, which represents SOM associated with the mineral phase.

Soil P_{org} compounds are an intrinsic part of SOM. Hence, further studies on soil P_{org} should include state of the art research on SOM. We made an attempt in this study by combining the Humeomics SOM fractionation procedure with solution ^{31}P NMR spectroscopy. However, we were only able to investigate one soil due to the laborious extraction and analysis procedures. Reducing complexity by e.g. removing the KOH in MeOH extraction is necessary in order to test the method on a variety of soils with diverse P_{org} compositions.

Declaration of Competing Interest

The authors declare the following financial interests/personal relationships which may be considered as potential competing interests: Jolanda Reusser reports financial support was provided by Swiss National Science Foundation.

Data availability

Data will be made available on request.

Acknowledgements

We would like to acknowledge Dr Laurie Paule Schönholzer, Dr Federica Tamburini, Ms Monika Macsai, and Dr Astrid Oberson for their technical support and discussions. Furthermore, the authors are thankful for the support provided by the whole CERMANU team at the University of Napoli Federico II in Italy. We gratefully acknowledge funding from the Swiss National Science Foundation, Switzerland [grant number 200021_169256].

Appendix A. Supplementary data

Supplementary data to this article can be found online at https://doi.org/10.1016/j.geoderma.2022.116227.

References

Anderson, G., 1980. Assessing organic phosphorus in soils. In: Khasawneh, F.E., Sample, E.C., Kamprath, E.J. (Eds.), The Role of Phosphorus in Agriculture. American Society of Agronomy, Crop Science Society of America, Soil Science Society of America, Madison, WI, pp. 411–431.

Blume, H.P., Brümmer, G.W., Scheffer, F., Horn, R., Kandeler, E., Schachtschabel, P., Kögel-Knabner, I., Welp, G., Kretzschmar, R., Thiele-Bruhn, S., 2009. Scheffer/Schachtschabel: Lehrbuch der Bodenkunde. Spektrum Akademischer Verlag.

Borie, F., Zunino, H., Martínez, L., 1989. Macromolecule-P associations and inositol phosphates in some Chilean volcanic soils of temperate regions. Commun. Soil Sci. Plant Analysis 20 (17–18), 1881–1894.

Cade-Menun, B.J., 2005. Characterizing phosphorus in environmental and agricultural samples by ^{31}P nuclear magnetic resonance spectroscopy. Talanta 66 (2), 359–371.

Cade-Menun, B.J., 2015. Improved peak identification in ^{31}P-NMR spectra of environmental samples with a standardized method and peak library. Geoderma 257–258, 102–114.

Cade-Menun, B.J., Liu, C.W., Nunlist, R., McColl, J.G., 2002. Soil and litter phosphorus-31 nuclear magnetic resonance spectroscopy. J. Environ. Qual. 31 (2), 457–465.
Celi, L., Barberis, E., 2007. Abiotic reactions of inositol phosphates in soil. In: Turner, B. L., Richardson, A.E., Mullaney, E.J. (Eds.), Inositol Phosphates: Linking Agriculture and the Environment. CABI, Wallingford, pp. 207–220.
Celi, L., Lamacchia, S., Marsan, F.A., Barberis, E., 1999. Interaction of inositol hexaphosphate on clays: adsorption and charging phenomena. Soil Sci. 164 (8).
Claridge, T.D.W., 2016. Chapter 2 - Introducing high-resolution NMR. In: Claridge, T.D. W. (Ed.), High-Resolution NMR Techniques in Organic Chemistry. Elsevier, Boston, pp. 11–59.
Condron, L.M., Turner, B.L., Cade-Menun, B.J., 2005. Chemistry and dynamics of soil organic phosphorus. In: Sims, J.T., Sharpley, A.N. (Eds.), Phosphorus: Agriculture and the Environment. Agronomy Monograph. American Society of Agronomy, Crop Science Society of America, and Soil Science Society of America, Madison, WI, pp. 87–121.
Cosgrove, D.J., Irving, G.C.J., 1980. Inositol phosphates: their chemistry, biochemistry and physiology. Studies in Organic Chemistry, 4. Amsterdam: Elsevier.
Doolette, A.L., Smernik, R.J., Dougherty, W.J., 2009. Spiking improved solution phosphorus-31 nuclear magnetic resonance identification of soil phosphorus compounds. Soil Sci. Soc. Am. J. 73 (3), 919–927.
Dougherty, W.J., Smernik, R.J., Bünemann, E.K., Chittleborough, D.J., 2007. On the use of hydrofluoric acid pretreatment of soils for phosphorus-31 nuclear magnetic resonance analyses. Soil Sci. Soc. Am. J. 71 (4), 1111–1118.
Drosos, M., Nebbioso, A., Mazzei, P., Vinci, G., Spaccini, R., Piccolo, A., 2017. A molecular zoom into soil Humeome by a direct sequential chemical fractionation of soil. Sci. Total Environ. 586, 807–816.
Fioroto, A.M., Kelmer, G.A.R., Albuquerque, L.G.R., César Paixão, T.R.L., Oliveira, P.V., 2017. Microwave-assisted digestion with a single reaction chamber for mineral fertilizer analysis by inductively coupled plasma optical emission spectrometry. Spectrosc. Lett. 50 (10), 550–556.
Frossard, E., Buchmann, N., Bünemann, E.K., Kiba, D.I., Lompo, F., Oberson, A., Tamburini, F., Traoré, O.Y.A., 2016. Soil properties and not inputs control carbon: nitrogen:phosphorus ratios in cropped soils in the long term. Soil 2 (1), 83–99.
George, T.S., Giles, C.D., Menezes-Blackburn, D., Condron, L.M., Gama-Rodrigues, A.C., Jaisi, D., Lang, F., Neal, A.L., Stutter, M.I., Almeida, D.S., Bol, R., Cabugao, K.G., Celi, L., Cotner, J.B., Feng, G., Goll, D.S., Hallama, M., Krueger, J., Plassard, C., Rosling, A., Darch, T., Fraser, T., Giesler, R., Richardson, A.E., Tamburini, F., Shand, C.A., Lumsdon, D.G., Zhang, H., Blackwell, M.S.A., Wearing, C., Mezeli, M. M., Almås, Å.R., Audette, Y., Bertrand, I., Beyhaut, E., Boitt, G., Bradshaw, N., Brearley, C.A., Bruulsema, T.W., Ciais, P., Cozzolino, V., Duran, P.C., Mora, M.L., de Menezes, A.B., Dodd, R.J., Dunfield, K., Engl, C., Frazão, J.J., Garland, G., González Jiménez, J.L., Graca, J., Granger, S.J., Harrison, A.F., Heuck, C., Hou, E.Q., Johnes, P.J., Kaiser, K., Kjær, H.A., Klumpp, E., Lamb, A.L., Macintosh, K.A., Mackay, E.B., McGrath, J., McIntyre, C., McLaren, T., Mészáros, E., Missong, A., Mooshammer, M., Negrón, C.P., Nelson, L.A., Pfahler, V., Poblete-Grant, P., Randall, M., Seguel, A., Seth, K., Smith, A.C., Smits, M.M., Sobarzo, J.A., Spohn, M., Tawaraya, K., Tibbett, M., Voroney, P., Wallander, H., Wang, L., Wasaki, J., Haygarth, P.M., 2018. Organic phosphorus in the terrestrial environment: a perspective on the state of the art and future priorities. Plant Soil 427 (1), 191–208.
Goh, K.M., Williams, M.R., 1982. Distribution of carbon, nitrogen, phosphorus, sulphur, and acidity in two molecular weight fractions of organic matter in soil chronosequences. J. Soil Sci. 33 (1), 73–87.
Harrison, H.F., 1987. Soil Organic Phosphorus: A Review of World Literature. CAB International, Wallingford.
He, Z., Ohno, T., Cade-Menun, B.J., Erich, M.S., Honeycutt, C.W., 2006. Spectral and chemical characterization of phosphates associated with humic substances. Soil Sci. Soc. Am. J. 70 (5), 1741–1751.
Hochberg, Y., Tamhane, A.C., 1987. Multiple Comparison Procedures. Wiley Series in Probability and Mathematical Statistics. Applied Probability and Statistics, Wiley, New York.
Hong, J.K., Yamane, I., 1980. Inositol phosphate and inositol in humic acid and fulvic acid fractions extracted by three methods. Soil Sci. Plant Nutr. 26 (4), 491–505.
Jarosch, K.A., Doolette, A.L., Smernik, R.J., Tamburini, F., Frossard, E., Bünemann, E.K., 2015. Characterisation of soil organic phosphorus in NaOH-EDTA extracts: a comparison of ^{31}P NMR spectroscopy and enzyme addition assays. Soil Biol. Biochem. 91, 298–309.
John, M.K., Sprout, P.N., Kelley, C.C., 1965. The distribution of organic phosphorus in British Columbia soils and its relationship to soil characteristics. Can. J. Soil Sci. 45 (1), 87–95.
Jørgensen, C., Turner, B.L., Reitzel, K., 2015. Identification of inositol hexakisphosphate binding sites in soils by selective extraction and solution ^{31}P NMR spectroscopy. Geoderma 257–258, 22–28.
Kleber, M., Sollins, P., Sutton, R., 2007. A conceptual model of organo-mineral interactions in soils: self-assembly of organic molecular fragments into zonal structures on mineral surfaces. Biogeochemistry 85 (1), 9–24.
Kögel-Knabner, I., 1997. ^{13}C and ^{15}N NMR spectroscopy as a tool in soil organic matter studies. Geoderma 80 (3), 243–270.
Kögel-Knabner, I., de Leeuw, J.W., Hatcher, P.G., 1992. Nature and distribution of alkyl carbon in forest soil profiles: implications for the origin and humification of aliphatic biomacromolecules. Sci. Total Environ. 117–118, 175–185.
Mazzei, P., Piccolo, A., 2015. Interactions between natural organic matter and organic pollutants as revealed by NMR spectroscopy. Magn. Reson. Chem. 53 (9), 667–678.
McCarthy, S.M., Melman, J.H., Reffell, O.K., Gordon-Wylie, S.W., 2020. Chapter 24 - Synthesis and partial characterization of biodiesel via base-catalyzed transesterification. In: Dahiya, A. (Ed.), Bioenergy (Second Edition). Academic Press, pp. 519–524.
McDowell, R.W., Stewart, I., 2006. The phosphorus composition of contrasting soils in pastoral, native and forest management in Otago, New Zealand: sequential extraction and ^{31}P NMR. Geoderma 130 (1), 176–189.
McLaren, T.I., Smernik, R.J., McLaughlin, M.J., McBeath, T.M., Kirby, J.K., Simpson, R. J., Guppy, C.N., Doolette, A.L., Richardson, A.E., 2015. Complex forms of soil organic phosphorus–A major component of soil phosphorus. Environ. Sci. Technol. 49 (22), 13238–13245.
McLaren, T.I., Verel, R., Frossard, E., 2019. The structural composition of soil phosphomonoesters as determined by solution ^{31}P NMR spectroscopy and transverse relaxation (T_2) experiments. Geoderma 345, 31–37.
McLaren, T.I., Smernik, R.J., McLaughlin, M.J., Doolette, A.L., Richardson, A.E., Frossard, E., 2020. Chapter Two - The chemical nature of soil organic phosphorus: a critical review and global compilation of quantitative data. In: Sparks, D.L. (Ed.), Advances in Agronomy. Academic Press, pp. 51–124.
Milliken, G.A., Johnson, D.E., 2009. Analysis of messy data. Volume 1: designed experiments. 2nd ed. Boca Raton, Fla: CRC Press.
Moyer, J.R., Thomas, R.L., 1970. Organic phosphorus and inositol phosphates in molecular size fractions of a soil organic matter extract. Soil Sci. Soc. Am. J. 34(1), 80-83.
Nebbioso, A., Piccolo, A., 2011. Basis of a Humeomics Science: chemical fractionation and molecular characterization of humic biosuprastructures. Biomacromolecules 12 (4), 1187–1199.
Nebbioso, A., Vinci, G., Drosos, M., Spaccini, R., Piccolo, A., 2015. Unveiling the molecular composition of the unextractable soil organic fraction (humin) by humeomics. Biol. Fertil. Soils 51 (4), 443–451.
Neptune, A.M.L., Tabatabai, M.A., Hanway, J.J., 1975. Sulfur fractions and carbon-nitrogen-phosphorus-sulfur relationships in some Brazilian and Iowa soils. Soil Sci. Soc. Am. J. 39 (1), 51–55.
Ognalaga, M., Frossard, E., Thomas, F., 1994. Glucose-1-phosphate and *myo*-inositol hexaphosphate adsorption mechanisms on goethite. Soil Sci. Soc. Am. J. 58 (2), 332–337.
Ogner, G., 1983. ^{31}P-NMR spectra of humic acids: a comparison of four different raw humus types in Norway. Geoderma 29 (3), 215–219.
Ohno, T., Zibilske, L.M., 1991. Determination of low concentrations of phosphorus in soil extracts using malachite green. Soil Sci. Soc. Am. J. 55 (3), 892–895.
Piccolo, A., 2001. The supramolecular structure of humic substances. Soil Sci. 166 (11).
Piccolo, A., 2012. Carbon Sequestration in Agricultural Soils: A Multidisciplinary Approach to Innovative Methods. Springer, Berlin, Heidelberg.
Piccolo, A., Spaccini, R., Savy, D., Drosos, M., Cozzolino, V., 2019. The soil humeome: chemical structure, functions and technological perspectives. In: Vaz, S. (Ed.), Sustainable Agrochemistry - A Compendium of Technologies. Springer International Publishing, pp. 183–222.
Reusser, J.E., Verel, R., Frossard, E., McLaren, T.I., 2020a. Quantitative measures of *myo*-IP_6 in soil using solution ^{31}P NMR spectroscopy and spectral deconvolution fitting including a broad signal. Environ. Sci. Processes Impacts 22 (4), 1084–1094.
Reusser, J.E., Verel, R., Zindel, D., Frossard, E., McLaren, T.I., 2020b. Identification of lower-order inositol phosphates (IP_5 and IP_4) in soil extracts as determined by hypobromite oxidation and solution ^{31}P NMR spectroscopy. Biogeosciences 17 (20), 5079–5095.
Schmidt, M.W.I., Torn, M.S., Abiven, S., Dittmar, T., Guggenberger, G., Janssens, I.A., Kleber, M., Kögel-Knabner, I., Lehmann, J., Manning, D.A.C., Nannipieri, P., Rasse, D.P., Weiner, S., Trumbore, S.E., 2011. Persistence of soil organic matter as an ecosystem property. Nature 478 (7367), 49–56.
Simpson, M.J., Simpson, A.J., 2017. NMR of soil organic matter. In: Lindon, J.C., Tranter, G.E., Koppenaal, D.W. (Eds.), Encyclopedia of Spectroscopy and Spectrometry, Third Edition. Academic Press, Oxford, pp. 170–174.
Smernik, R.J., Dougherty, W.J., 2007. Identification of phytate in phosphorus-31 nuclear magnetic resonance spectra: the need for spiking. Soil Sci. Soc. Am. J. 71 (3), 1045–1050.
Spaccini, R., Mbagwu, J.S.C., Conte, P., Piccolo, A., 2006. Changes of humic substances characteristics from forested to cultivated soils in Ethiopia. Geoderma 132 (1), 9–19.
Stevenson, F.F., 1986. Cycles of Soil: Carbon, Nitrogen, Phosphorus, Sulfur, Micronutrients. A Wiley-Interscience publication, John Wiley and Sons, New York.
Stevenson, F.J., 1994. Humus Chemistry: Genesis, Composition, Reactions, Second ed. Wiley, New York [etc.].
Strickland, K.P., 1973. The Chemistry of Phospholipids. Form and Function of Phospholipids, 3. Second, completely revised and enlarged edition. ed. Elsevier Scientific Publ. Company.
Tipping, E., Somerville, C.J., Luster, J., 2016. The C:N:P: S stoichiometry of soil organic matter. Biogeochemistry 130 (1), 117–131.
Turner, B.L., Papházy, M.J., Haygarth, P.M., McKelvie, I.D., 2002. Inositol Phosphates in the Environment. Philos. Trans. R. Soc. London. Series B: Biol. Sci. 357(1420), 449.
Turner, B.L., Mahieu, N., Condron, L.M., 2003. Quantification of *myo*-inositol hexakisphosphate in alkaline soil extracts by solution ^{31}P spectroscopy and spectral deconvolution. Soil Sci. 168 (7), 469–478.
Turner, B.L., Richardson, A.E., 2004. Identification of *scyllo*-inositol phosphates in soil by solution phosphorus-31 nuclear magnetic resonance spectroscopy. Soil Sci. Soc. Am. J. 68 (3), 802–808.
Veinot, R.L., Thomas, R.L., 1972. High molecular weight organic phosphorus complexes in soil organic matter: inositol and metal content of various fractions. Soil Sci. Soc. Am. J. 36 (1), 71–73.
WRB, I.W.G., 2014. World Reference Base for Soil Resources. International Soil Classification System for Naming Soils and Creating Legends for Soil Maps. World Soil Resources Reports No. 106. Food and Agriculture Organization of the United Nations FAO, Rome.